Accepted Manuscript

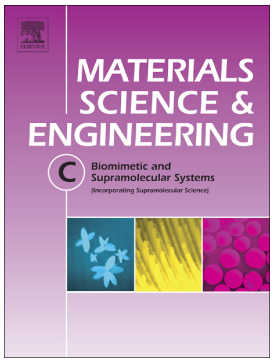

ZnO nanoflower based sensitive nano-biosensor for amyloid detection

Najim Akhtar, Sanjay Kisan Metkar, Agnishwar Girigoswami, Koyeli Girigoswami

PII: S0928-4931(17)31148-7
DOI: doi: 10.1016/j.msec.2017.04.118
Reference: MSC 7941

To appear in: *Materials Science & Engineering C*

Received date: 27 March 2017
Revised date: 17 April 2017
Accepted date: 19 April 2017

Please cite this article as: Najim Akhtar, Sanjay Kisan Metkar, Agnishwar Girigoswami, Koyeli Girigoswami , ZnO nanoflower based sensitive nano-biosensor for amyloid detection. The address for the corresponding author was captured as affiliation for all authors. Please check if appropriate. Msc(2017), doi: 10.1016/j.msec.2017.04.118

This is a PDF file of an unedited manuscript that has been accepted for publication. As a service to our customers we are providing this early version of the manuscript. The manuscript will undergo copyediting, typesetting, and review of the resulting proof before it is published in its final form. Please note that during the production process errors may be discovered which could affect the content, and all legal disclaimers that apply to the journal pertain.

ACCEPTED MANUSCRIPT

ZnO Nanoflower Based Sensitive Nano-biosensor for Amyloid Detection

Najim Akhtar, Sanjay Kisan Metkar, Agnishwar Girigoswami and Koyeli Girigoswami

Medical Bionanotechnology Laboratory, Faculty of Allied Health Sciences, Chettinad Academy of Research and Education (CARE), Chettinad Health City, Kelambakkam, Chennai-603103, India

*To whom correspondence should be addressed: koyelig@gmail.com;

Telephone: +91-9600060358.

Running title: ZnO nanoflower based amyloid sensor.

ACCEPTED MANUSCRIPT

ACCEPTED MANUSCRIPT

Abstract

Zinc oxide (ZnO) is a semiconductor metal oxide nanoparticle with inherent optical properties. Among the different zinc oxide nanostructures, nanoflowers have greater surface area. Utilizing this property a reagentless biosensor has been developed for the detection of beta amyloids, a hallmark of neurodegenerative diseases like Alzheimer's disease, Creutzfeldt-Jakob Syndrome, insulin dependent type II diabetes etc. The poor fluorescence quantum yield and photobleaching effect of Thioflavin T (ThT) upon binding to the model insulin amyloid beta sheets in solution can be overcome by the present engineered biosensor where ThT acts as a target as well as a reporter to detect amyloids adsorbed on a solid template based on ZnO nanoflower. ThT was adsorbed on ZnO NFs grown over nano-silver thin film coated glass slide. The *in vivo* imaging system was used to detect and quantify the fluorescence intensity generated from the substrates upon binding with insulin amyloid. ZnO NFs have the waveguiding property which increases the local field intensity caused by a resonance between the guided fundamental mode and evanescent field associated with high- order modes. This resonance phenomenon reinforces the excitation of the fluorophores in close proximity of the NFs thereby exhibiting enhanced fluorescence like Fabry Pero´t Resonator (FPR). Considering the engineering and sensitivity, the reported nanobiosensor developed on ZnO nanoflower can be treated as faster and cost effective amyloid sensor.

Keywords: ZnO nanoflower; amyloid detection; insulin amyloid; amyloidosis.

ACCEPTED MANUSCRIPT

1. Introduction

Amyloids are the misfolded protein aggregates having predominant crossed β-sheet rich structures typically found in different diseased conditions called amyloidosis. Amyloids are associated with various neurodegenerative disorders like Alzheimer's disease (AD) (1, 2), Parkinson's disease (PD) (3), Creutzfeldt- Jakob Disease (CJD), Prion- associated diseases (4) as well as Type II diabetes (5, 6). Insulin injections are taken subcutaneously in type II diabetic patients chronically. The repeated use of such injections induces localized amyloidosis. These insulin amyloids also share the same β-sheet rich structure as other amyloids (5) and are considered as a model amyloid protein for the study of different amyloidosis. The detection of amyloids in biological fluids at a very low concentration is warranted for the diagnosis and treatment of different amyloid related disorders. In the present study, we have developed a nanobiosensor for the detection of amyloids designed with zinc oxide (ZnO) nanoflower grown on various substrates and compared the efficacy. Fluorescent dyes are commonly used for labeling and detection of various disease biomarkers such as IgG, β-Amyloid etc., but has limitations in terms of low intensities and photo-stability. Nanostructures based ZnO nanorods are being used recently for fluorescence enhancement (FE) (7, 8), exploiting the large surface area of ZnO nanorods (8), interfacial electron transfer (9), and their waveguide structures (10-12). The fluorescence from the fluorophores near nanorods can be captured and guided by waveguide structures (13). To achieve the enhanced fluorescence, we have grown ZnO nanoflower with ZnO nanoparticles as seed, which has higher surface area compared to ZnO nanorod, over a high reflectance substrate coated with nano silver (Ag) thin film.

The detection of amyloid so far is very laborious, time consuming and involves expensive chemicals and very less sensitive. Biochemical techniques like ELISA and mass spectrometry

ACCEPTED MANUSCRIPT

(MS) is been used for the quantification of amyloid-beta peptides present in the brains of humans and transgenic mice (14). ELISA can detect as low as picomolar concentrations of amyloid beta (15) but involves expensive enzyme-linked antibody and a carcinogenic substrate. Amyloid detection using MS yields less reliable results because of robust MS methods, low sensitivity, self-aggregation, difficulties in purification, and adsorption in the sample vials, injector ports, and the chromatographic columns etc. (16). The recent techniques of detection of amyloids are- on-line immunoaffinity liquid chromatography–mass spectrometry (LC/MS/MS) (17), column-switching liquid chromatographic–tandem mass spectrometry (18), time-of-flight secondary ion mass spectrometry (19) and covalent chiral derivatized ultraperformance liquid chromatography tandem mass spectrometry (CCD-UPLC–MS/MS) (20). These techniques are time-consuming, expensive, labor intensive, and their sensitivity is also compromised. Positron emission tomography (PET) is used to detect amyloid β (Aβ) with only three Aβ PET tracers approved by the Food and Drug Administration (FDA) for clinical applications (21). The disadvantages of these three tracers and other tracers which are under development is that they can bind to the insoluble Aβ but not to the more toxic soluble oligomeric Aβ species (22). The detection of soluble Aβ peptide is more essential for the early detection of AD. A non fluorescent peptide tagged with green fluorescence molecule was used to detect amyloids and was considered superior to the conventional ThT assay but had a high signal to noise ratio (23). There were other studies on the influence of small peptides on amyloid aggregation where the fibrillar morphology of amyloids was visualized using atomic force microscopy (AFM), but no quantifications were done (24).

The use of benzothiazole dyes, mostly thioflavin T (ThT) as whole or part is used for the detection of amyloids through histological, imaging, kinetic, and structural studies (25, 26).

ACCEPTED MANUSCRIPT

Organic fluorophores have a limitation because it does not give a reproducible signal for amyloid detection at low concentration. In our present work, we have adsorbed ThT dye over ZnO nanoflower grown over a nano Ag thin film coated glass surface. Insulin amyloids were used for the detection of amyloids using the enhanced fluorescence emitted from this fabricated nanobiosensor. The linearity of the sensor is also verified using different concentrations of the amyloid and yielded a cost effective, faster and sensitive amyloid biosensor. The characterization of the nanostructure was done using UV visible spectroscopy, spectrofluorimetry, dynamic light scattering (DLS), infrared spectroscopy (FTIR), X-ray diffractometry (XRD) and scanning electron microscopy (SEM). The fluorescence emitted from the fabricated sensor is recorded using IVIS Lumia live small animal imaging system.

2. Materials and methods

2.1 Glass slide preparation and surface treatment

The glass slides activation and surface treatment was done according to previously described methods by Chitvoranund N *et al.,* (27). Briefly, all glass slides of size 3×1 inch were dipped in distilled water and ultrasonicated for 5 min in the water bath at 40 KHz frequency. Then, the glass slides were further dipped in 95 % ethanol and ultrasonicated for 5 min and the process was repeated three times for activation. The glass slides were air dried and dipped in 1 M hydrofluoric (HF) acid for HF etching. After washing with distilled water the slides were air dried in a dirt free atmosphere.

2.2 Electroless deposition of nano-Ag thin film

Nano Ag thin film was deposited over the activated glass by following method used by Koura N *et al.,* (28), with few modifications. 20 ml of 1 % silver nitrate ($AgNO_3$) was mixed

ACCEPTED MANUSCRIPT

with 1 % sodium hydroxide (NaOH) under continuous stirring to form a fine green solution of Ag_2O. After 5 minutes of stirring 1 ml of ammonia solution was added dropwise until a colorless solution was obtained. In the above solution, 2 g of D-glucose was added under stirring condition. Next, the HF activated glass slides was immersed in that solution and held for different time intervals in order to standardize the optimum thickness of the film. After nano Ag thin film deposition the glass slides were gently rinsed with distilled and annealed for 10 min at 120 °C.

2.3 Zinc oxide nanoparticles synthesis

Zinc oxide nanoparticles (ZnO NPs) were synthesized using simple beaker chemistry as followed by Ghorbani H. R *et al.* (29), with slight modifications. To the aqueous solution (0.2 M) of zinc nitrate ($Zn(NO_3)_2.6H_2O$), KOH (0.4 M) solution was added dropwise with continuous stirring at room temperature. Upon addition of KOH, the solution yielded a white colored precipitate which was centrifuged at 5000 rpm for 20 min followed by distilled water washing for three times. The final washing was done with 95 % ethanol to remove the interfering chemicals and the final product was calcinated at 500 °C for 3 h. The white powder was then grinded in a mortar pestle to yield a fine powder of ZnO NPs. The characterization of the nanoparticles was done using UV-visible absorbance, fluorescence, FTIR, particle size analysis and XRD according to Girigoswami K *et al.* (30).

2.4 Seeding of ZnO NPs

Spin coating of ZnO nanoparticles was done as described by Ibupoto Z H *et al.* (31). At first ZnO NPs seed solution was prepared with ZnO NP in 1% acetic acid solution followed by ultrasonication for 30 min. The nano Ag- coated and uncoated slides were then spin coated with

ACCEPTED MANUSCRIPT

the seed solution of ZnO NPs at 3000 rpm for 30 s, three times. The substrates were then annealed at 120 °C for 20 min, after seeding.

2.5 Growth of ZnO nanoflower on substrates

ZnO nanoflowers (NFs) were grown on the seeded substrates by following the method used by Khun K *et al.* (32) with slight modification. Aqueous solutions of zinc nitrate hexahydrate (75 mM) and hexamethylenetetramine (HMT) (75 mM) was prepared and 30 ml of each solution was mixed in a beaker to yield the growth solution. To this growth solution, the annealed substrates were dipped vertically and kept in a preheated water bath at 96 °C for 5 h. After 5 h the growth solution was replaced with fresh growth solution and kept for another 5 h at the same condition. After complete growth process of ZnO NFs, the substrates were washed with distilled water, followed by air drying.

2.6 Adsorption of Thioflavin T on different substrates

The solution of 20 μM ThT was prepared in PBS (pH=7.2). The adsorption of dye to a substrate was done according to Yin Y *et al.*, 2014 (13). In a coplin jar 30 ml of ThT solution was taken and four different types of substrate, Only Glass (activated glass slide), Substrate-A (ZnO NFs grown on activated glass slide), Substrate-B (nano Ag coated glass slide) and Substrate-C (ZnO NFs grown on nano Ag coated glass slide) was immersed into it and kept at 4 °C for 12 h. Then, the ThT adsorbed substrates were air dried in a dirt free atmosphere.

2.7 Growth of insulin amyloid and its confirmation

To analyze the detection capacity of the ThT adsorbed surface, insulin amyloids were used. The insulin amyloids were formed *in vitro* according to Metkar S K *et al.*, (33). 1 ml of Huminsulin

ACCEPTED MANUSCRIPT

(1.388 mg/ml) was taken in a 2 ml tube and incubated at 65 °C (wet heat) for 24 h. After the incubation, amyloid fibril formation was confirmed by conventional ThT fluorescence assay in solution (34). In a typical ThT assay, 30 µl of insulin amyloid was added in 200 µl of ThT (20 µM). From this solution, 20 µl was further added in 3 ml distilled water and the fluorescence spectra was recorded at excitation 412 nm (absorption peak of ThT) and emission 478 nm (33). BSA was taken as an example of non amyloidogenic protein in previous studies (34). BSA at a concentration similar to insulin amyloid was taken as a negative control. 1 ml of 1.4 mg/ml BSA solution was prepared and 30 µl of BSA solution was mixed with 200 µl of 20 µM ThT solution. From the above solution, 20 µl was added in 3 ml distilled water and the fluorescence spectra were recorded in a similar way as described above.

2.8 Detection of insulin amyloid on different substrates using *in vivo* imaging system:

Three sets of ThT adsorbed substrates was taken and marked as set-1, set-2 and set-3. Each set containing four substrates, one from each type (Only glass, Substrate A, Substrate B and Substrate C). Then before adding the sample all the substrates was arranged on the sample stage-D (1.5 cm) of Lumina IVIS and the fluorescence image was acquired using the excitation filter as GFP (Green Fluorescent Protein) (excitation at 430 nm and emission from 480 nm) (33). After taking the fluorescence image all the substrates was taken out and the set-1 substrates were left as blank. 10 µl of BSA (1.4 mg/ml) solution was added to set-2 and 10 µl of insulin amyloid was added to set-3. After sampling, the substrates were kept at room temperature for 15 min and fluorescence images were captured in the same manner. All the experiments were conducted in a dark room and repeated three times. The quantification of the amount of fluorescence was done by obtaining the fluorescence of the region of interest (ROI) of each substrate.

ACCEPTED MANUSCRIPT

2.9 Linearity of Substrate-C as amyloid sensor

To five Substrate-C, five different amount of insulin amyloid (02 µl, 05 µl, 10 µl, 20 µl and 40 µl respectively) was added and the fluorescence images were acquired using Lumina IVIS. The ROI was selected and the fluorescence intensity was quantified to compare in between the different amount of amyloid added.

3. Results

3.1 Characterization of zinc oxide nanoparticles (ZnO NPs)

Fig 1 (A) shows the UV – visible spectrum of the synthesized ZnO NP. The SPR band centered at 368.8 nm confirms the formation of ZnO nanoparticles with a band gap of 3.17 eV and that indicates the semiconducting nature of ZnO NP. The fluorescence emission maxima peaked at 394 nm upon excitation at 368 nm Fig 1 (B). The FTIR spectrum of ZnO NP was recorded in transmittance mode and the characteristic bands were noted (Fig 1 (C)). The IR spectrum peaks are given in Table I and confirms the presence of ZnO nanoparticles.

Table I: FTIR spectral characteristics of ZnO NPs

IR Band (cm^{-1})	Description
2906.13	C-H stretching vibration
1663.66	C=O symmetric stretching vibration
1384.05	C=O asymmetric C=O stretching vibration
841.75	Due to the formation of tetrahedral coordination of Zn.

ACCEPTED MANUSCRIPT

915.69	C-O stretching vibration
762.39	Attributed to the C-O bond stretching
653.27 and 692.95	Indicates the stretching vibrations of ZnO NPs

The size distribution of synthesized ZnO NPs was determined using DLS analysis (Fig 1 (D)). The major scattering peak obtained for synthesized ZnO NPs at 380 nm indicating the hydrodynamic diameter of the NPs. The X-ray diffraction patterns (Fig 1 (E)) of ZnO NPs were obtained at 2θ = 34.4192°, 37.739°, 36.2185°, 47.421° and 56.561° are associated with lattice parameters (hkl) of (002), (100), (101), (102) and (110). The (hkI) values are agreed well with the standard JCPDS pattern of ZnO powder sample (JCPDS file No: 36- 1451). The mean crystallite size (D) of the prepared ZnO NP was calculated by using Debye-Scherrer's formula (30).

$$D = 0.9\,\lambda/\beta\cos\theta$$

Where,

λ = the wavelength of X-rays used (1.54060 Å), β = the full width at half maximum (FWHM) and θ = the angle of diffraction.

The mean crystallite size of the prepared ZnO nanopowder is calculated to be 18 nm.

3.2. Fabrication of amyloid sensor

The electroless deposition of nano Ag thin film coating was done using simple wet chemistry yielding a fine Ag layer on activated glass substrate (Fig 2(A)). UV-visible spectroscopy confirms the Ag thin film coating (Fig 2(B)) and the morphology of thin film were determined by SEM (Fig 2(C)). The SEM image of the nano Ag thin film shows a uniform coating of Ag throughout

ACCEPTED MANUSCRIPT

the surface with the metallic shine. The activated glass substrates and nano Ag coated activated glass substrates were then spin coated with a seed layer of ZnO NPs and ZnO NFs were grown above the ZnO seeded layer. Deposition of seed layer was confirmed by SEM (Fig 3A). The ZnO NPs are indicated with red circles and is found to be seeded in the thin nano Ag layer. The SEM image of ZnO NFs that were physically etched out from the one grown over glass substrate and the SEM images of ZnO NFs grown on activated glass substrate via hydrothermal method is shown in Fig 3B and Fig 3C respectively. The SEM picture of the nanoflowers shows the formation of nanoflowers with the petals in the shape of hexagonal rods. The SEM of ZnO NFs grown on Ag coated activated glass substrate is shown in Fig 3D indicating that the nano Ag thin film is not altered after the flower growth. The SEM images give the structural confirmations of grown ZnO NFs over different substrates and the shape of the flower petals are hexagonal cylinders which are grown from a ZnO core. The whole fabrication process was schematically represented in Fig 4. The target fluorophore, ThT, was the allowed to adsorb over the ZnO NFs and the analyte (insulin amyloid) was added over it. The fluorescence image (Fig 4 G) was taken using Lumina IVIS.

3.3 Growth of insulin amyloid

The growth of insulin amyloid in solution was confirmed by conventional ThT assay (Fig S1). The fluorescence spectrum of ThT along with the grown insulin amyloid fibrils was compared with ThT alone. The increment in intensity of emission spectra was observed in the case of ThT with insulin amyloid whereas the non-amyloid protein, BSA, did not show any increment in the fluorescent intensity upon binding with ThT.

3.4 Insulin amyloid detection using various substrates

ACCEPTED MANUSCRIPT

The fluorescence image of various substrates; Only Glass (activated glass slide), Substrate-A (ZnO NFs grown on activated glass slide), Substrate-B (Ag coated glass slide) Substrate-C (ZnO NFs grown on Ag coated glass slide), with and without insulin amyloid and BSA were taken by Lumina i*n-vivo* animal imaging system and the fluorescence intensity was recorded by selecting ROI (region of interest).

The fluorescence images of Only Glass substrates without and with insulin amyloid binding, and the fold increase in fluorescence intensity is shown in Fig 5-I (A) and Fig 5-I (B) respectively. The fluorescence intensity was not changed as visualized and the fold increase in the fluorescence intensity was 1.1 times which insignificant ($p \leq 0.001$). The images of fluorescence emitted from bare Substrate A, upon BSA binding and upon insulin amyloid binding respectively is shown in Fig 5-II (A). The increase in fluorescence intensity was found to be 2.7 fold higher (Fig 5-II (B)) upon insulin amyloid binding compared to bare Substrate-A. However, binding of BSA to Substrate-A did not increase the fluorescent intensity (0.95 fold) significantly ($p \leq 0.001$). The fluorescent detection of insulin amyloid using Substrate-B is shown in Fig 5-III (A). Upon insulin amyloid binding, the increment in the fluorescence intensity was about 1.31 times (Fig 5-III (B)). Fig 5-IV (A) shows the fluorescence images captured for bare Substrate-C, upon BSA binding and upon insulin amyloid binding respectively. The fold increase in fluorescence intensity upon binding with BSA and insulin amyloid respectively is shown in Fig 5-IV (B). There was an increment in the fluorescence intensity after binding with insulin amyloid (2.71 fold).

3.5 Fold increase in fluorescence intensity from different substrates

ACCEPTED MANUSCRIPT

In the various substrates same amount (10 µl) of insulin amyloid was given and fluorescence images were interpreted. It was observed that the maximum fluorescence intensity was produced by Substrate-C (Fig 6). Compared to Only Glass, 9.81±0.29 fold higher fluorescence signals were produced by Substrate-C.

3.6 Linearity of Substrate-C as amyloid sensor

Substrate-C was found to be an efficient amyloid sensor compared to other substrate and its linearity was studied using fluorescence imaging. Before and after adding different amount of insulin amyloid in different Substrate-C, the fluorescence images were taken (Fig 7 (A)) and the fluorescence intensity for different amounts of insulin amyloid was plotted (Fig 7 (B)).

4. Discussion

Biosensors have captured a huge market in the field of bionanotechnology exploiting the unique properties of nanostructures to their bulk counterparts. Several sensing mechanisms are being developed using different molecules, microbes, enzymes, DNA, proteins, peptides, cells etc. to detect the desirable end points. Our present study exploits the nanostructure developed by ZnO NFs grown on various substrates and comparing the efficacy of the substrates to act as a sensitive amyloid biosensor. Amyloids are the misfolded protein aggregates found in the pathophysiological conditions of the individuals with amyloidosis. The proteins responsible for amyloidosis are present in soluble form in normal individuals but get converted to its insoluble form at the time of the diseased condition. The reason behind the transformation of normally soluble proteins to its abnormally misfolded insoluble form is still unknown. Thus, to detect these insoluble amyloids in biological fluids can lead to an early prevention of the onset of

ACCEPTED MANUSCRIPT

amyloidosis. In the present study, we have taken insulin amyloid as our analyte which we wanted to detect by our fabricated amyloid sensor.

ZnO NPs were synthesized using zinc nitrate hexahydrate as a precursor by co-precipitation method and characterized biophysically. The absorbance peak, fluorescence emission, FTIR peaks and XRD pattern (Fig 1) concluded that the synthesized nanoparticle was ZnO NP with typical metal oxide semiconductor properties. These nanoparticles were used as a seed for ZnO NF growth. Previous studies have shown a typical absorption band around 370 nm corresponds to ZnO NPs (29, 30). To prepare different substrates for comparison of efficacy of fluorescence enhancement, glass slides were HF activated and then coated with nano Ag thin film. Ag, at its nanoscale has large reflectance and can enhance fluorescence by acting as a reflecting mirror. On the other hand, the bare glass substrate has high refractive index which enables it to absorb most of the UV light falling on it for the sensor application. This limitation is overcome by Ag thin film coating on glass substrate (13). Studies have also shown that Ag nanostructure can directly contribute to enhance fluorescence (35, 36). Thus, compared to bare glass, Ag thin film coated glass can be effective in enhancing even a small amount of fluorescent signal. The typical snapshot of Ag thin film over activated glass substrate (Fig 2(A)) shows a uniform coating and mirror formation over the sensor region of 1 inch × 1 inch. The absorption spectrum of Ag thin film coated at different time intervals (Fig 2 (B)) shows a typical absorption peak at 370 nm corresponding to Ag thin films on solid substrates (37). As the time of coating increases the intensity of absorption also increases revealing that with an increase in time the thickness of the nano Ag thin film increases, not the particle size of the constituent Ag nanoparticles. We have typically selected the nano Ag thin film that is deposited at 10 min for our further studies. To grow ZnO NFs, the bare glass and the nano Ag thin film coated glass were seeded with ZnO

ACCEPTED MANUSCRIPT

NPs. The SEM image of ZnO NP seeded nano Ag thin film coated glass substrate (Fig 3(A)) reveals the spherical nature of the ZnO NPs (marked as red circles) and confirms that the seeding was successful and ZnO NF can be grown. ZnO NFs were grown atop activated glass (Fig 3(C)) as well as Ag thin film coated glass (Fig 3(D)) and the structural stability of the nanoflowers was tested by scraping the ZnO NFs from the bare glass and observing their structure by SEM (Fig 3(B)). The SEM images show a typical growth of ZnO NFs with hexagonal tips that can act as reflecting mirrors of a Fabry-Pero´t Resonator (FPR). ZnO NFs have been synthesized by some researchers through solution route (38, 39), but the flower tip produced in such processes are either flake like or needle shaped respectively and thus not suitable to act like a FPR. To enhance the low intensity fluorescence signals, metal nanostructures are often coupled with fluorophores by the process called metal enhanced fluorescence (MEF). ZnO is a metal oxide that can be fabricated into various nanostructures such as nanorods (10), nanowires and nanobelts (40), nanotubes (41) and nanoflowers (42), but the nanoflowers with hexagonal tips are more promising to be used for MEF. ZnO nanoflowers have many shapes. Usually the petals of the nanoflowers are like sheets or needle shaped. We have synthesized hexagonal tipped flower petals which can act as a reflecting surface itself compared to needle shape which does not have any face to reflect light at its tip.

The fluorophore we have used in our study is ThT, which is highly specific to detect amyloids. ThT can bind to amyloids and increase the intensity of fluorescence whereas when it interacts with non amyloidogenic proteins the fluorescence is unaltered. In our study, we have induced fibrillation in insulin and confirmed its amyloid structure by monitoring the ThT fluorescence in solution using spectrofluorimeter (Fig S1). This insulin amyloid was taken as our analyte and ThT as the fluorophore and target. Our sensor is based on the coupling of two concepts for the

ACCEPTED MANUSCRIPT

enhancement of ThT fluorescence. The first is the metal enhanced fluorescence which can be achieved by immobilizing the fluorophore over ZnO NFs. The second concept is further enhancement of this signal by proximity with nano Ag thin film as it is known in earlier studies that Ag nanostructures have the capacity to increase fluorescence (43). We have compared the fluorescence intensity change of insulin amyloid at a particular concentration (10 µl of 1.388 mg/ml) upon binding with ThT adsorbed over (i) activated bare glass (Only Glass), (ii) ZnO NF grown over activated glass (Substrate-A), (iii) Ag thin film coated glass (Substrate-B) and (iv) ZnO NF grown on Ag thin film coated glass (Substrate-C). The schematic diagram of the synthesized amyloid nanosensor is shown in Fig 4. When a small amount of insulin amyloid (10 µl) is added to ThT adsorbed bare glass, there is no significant increment in fluorescence (1.11 times fold increase) (Fig 5 I (B)). This shows that the fluorescent signal obtained from this amount of insulin is almost undetectable. Our target is to increase this intensity to a reproducible amount that can be recorded. Next, to substrate B the same amount of insulin amyloid is added and it showed increment in the fluorescent signal (Fig 5 II(B)) that can be attributed to the wave guiding nature of the ZnO NFs. The wave guiding nature of the ZnO NFs increases the evanescent field, thereby increasing the fluorescence of the fluorophore. It is also seen that there is no increment in fluorescence intensity due to binding of ThT with BSA which proves the specificity of ThT binding towards the amyloids. To normalize the fluorescence increment contributed by only Ag thin film we have taken Substrate B containing ThT adsorbed over only Ag thin film. Upon binding with the same amount of insulin amyloid there is an increase in fluorescence (1.47 fold) (Fig 5 III(B)) which can be due to the enhancement caused by the fluorophore remaining at the vicinity of the Ag nanostructure. It has been proposed earlier that whenever there is a Ag nanostructure present near a fluorophore, its fluorescence increases (43).

ACCEPTED MANUSCRIPT

To further enhance the intensity of ThT fluorescence we have used Substrate C which is based on the dual concept of MEF caused by the ZnO NFs as well as Ag thin film based enhancement which can act as a reflecting mirror like that in a FPR. The local field intensity of the fluorophore in proximity of the ZnO NFs is increased due to the resonance caused by the waveguided fundamental modes and the evanescent field associated with higher-order modes that can eventually reinforce the excitation of the fluorophore which is near and adsorbed on the flower surface (44, 45) . This causes the fluorescence enhancement of ThT. The addition of reflecting surface to Ag thin film can also be due to the hexagonal end surfaces of the ZnO NFs that can also act as reflecting mirror. It is seen that the fluorescence has increased upon binding with the same amount of insulin amyloid to 2.6 fold compared to Ag thin film coated glass substrate (Fig 5 IV(B)). In this case also BSA did not increase any ThT fluorescence. Thus, on comparing in between the Only Glass, Substrate A, Substrate B and Substrate C, we have found that Substrate C could enhance the fluorescence of ThT up to 9.8 fold compared to Only Glass (Fig 6). These results make Substrate C suitable to be used as a sensitive amyloid sensor as it can detect the signal which is almost undetectable by bare glass based sensor and has the capacity to amplify the signal about 10 times.

A biosensor is valid only if it can detect the signals in a linear fashion with respect to increase in the concentration of the analyte. Our Substrate C is the sensitive amyloid sensor and we have checked its linearity by varying the amount of insulin amyloid to be detected. The biosensor is linearly sensitive up to an amount of 20 µl (of 1.388mg/ml) of insulin amyloid (Fig 7B). At 40 µl (of 1.388mg/ml) insulin, the intensity is lower than the linear part which can be due to saturation of ThT amount. The amount of ThT available for amyloid binding may not be sufficient to give signal. Thus, our sensor is sensitive for detection from 2 µl (of 1.388mg/ml) to 20 µl (of

ACCEPTED MANUSCRIPT

1.388mg/ml) of insulin amyloid. The detection by our sensor is 2.76 µg which is nearly comparable with other detection techniques like ELISA that can detect upto picomolar concentration of amyloid Aβ (15).

There are few techniques known to detect amyloids like- ELISA, Western Blot, mass spectroscopy, PET scan etc., but all these techniques have some limitations in some aspect or other. Thus, it is warranted to develop a technique which can detect amyloids with high sensitivity, faster, simple and cost effective. Our amyloid sensor can detect the amyloids with very high sensitivity, through nanostructure based enhanced fluorescence, by detecting a low amount of amyloid which is otherwise almost undetectable by a conventional substrate (Only Glass). We can thus propose a simple, sensitive, cost effective and a faster technique to detect amyloids using our fabricated biosensor.

5. Conclusion

The present study reveals the development of a sensitive biosensor for the detection of amyloids. Amyloids detection is warranted for an early diagnosis of different neurodegenerative disorders and can enable researchers for the possible treatment of such diseases. The sensor is based on the mechanism of fluorescence enhancement of ThT bound insulin by the waveguiding capacity of ZnO NFs by acting as reflecting mirror in Fabry-Perot Resonator. This enhanced signal is further increased due to the Ag thin film coating as nano Ag can also act as reflecting mirror rather than absorbing the UV light like bare glass. This both enhancement concept has yielded a successful ThT fluorescence based amyloid biosensor that has enhanced the intensity of fluorescence by 9.8 fold. The intensity of fluorescence has been quantified using Lumia IVIS. In future, the study is to be done using a fluorescence microscope that can make the use of the same sensor in a much

ACCEPTED MANUSCRIPT

cost effective manner. The future study can also be focused on adsorbing different dye on the same platform to detect other analytes.

Acknowledgement

The authors acknowledge gratefully the financial and infrastructural support provided by Chettinad Academy of Research and Education (CARE), Kelambakkam, Chennai-603103. SM thanks CARE and UGC for providing the fellowship.

References

1. Stefani M and Dobson C M (2003); Protein aggregation aggregate toxicity: new insights into protein folding, misfolding diseases biological evolution; *J. Mol. Med.*, 81, 678-699.
2. Fändrich M, Meinhardt J and Grigorieff N (2009); Structural polymorphism of Alzheimer Aβ and other amyloid fibrils; *Prion*, 3, 89-93.
3. Braak H and Braak E (1990); Cognitive impairment in Parkinson's disease: amyloid plaques, neurofibrillary tangles, and neuropil threads in the cerebral cortex. J Neural. Transm. Park. Dis. Dement. Sect.; 2, 45-57.
4. Kitamoto T, Tateishi J, Tashima T, Takeshita I, Barry R.A., DeArmond S.J,Prusiner S.B. (1986); Amyloid plaques in Creutzfeldt-Jakob disease stain with prion protein antibodies; Ann. Neurol. ; 20, 204-208.
5. Jiménez J L, Nettleton E J, Bouchard M, Robinson C V, Dobson C M and Saibil H R (2002); The protofilament structure of insulin amyloid fibrils; *Proc. Natl. Acad. Sci. U.S.A.*, 99, 9196-9201.
6. Shikama Y, Kitazawa J, Yagihashi N, Uehara O, Murata Y, Yajima N, Wada R and Yagihashi S (2010); Localized amyloidosis at the site of repeated insulin injection in a diabetic patient; *Intern. Med.*, 49, 397–401.

ACCEPTED MANUSCRIPT

7. Dorfman A, Kumar N and Hahm J (2006); Highly sensitive biomolecular fluorescence detection using nanoscale ZnO platforms; Langmuir, 22, 4890–4895.
8. Kim J, Kwon S, Park J-K and Park I (2014); Quantum dot-based immunoassay enhanced by high-density vertical ZnO nanowire array; Biosens. Bioelectron.; 55, 209–215.
9. Fu Y, Zhang J and Lakowicz J R (2012); Photophysical behaviors of single fluorophores localized on zinc oxide nanostructures; Int. J. Mol. Sci; 13, 12100-12112.
10. Adalsteinsson V, Parajuli O, Kepics S, Gupta A, Reeves W A and Hahm J I (2008); Ultrasensitive detection of cytokines enabled by nanoscale ZnO arrays. Anal.Chem; 80, 6594–6601.
11. Wells S M, Merkulov I A, Kravchenko I I, Lavrik N V and Sepaniak M J (2012); Silicon nanopillars for field-enhanced surface spectroscopy; ACS Nano; 6, 2948–2959.
12. Seo K, Wober M, Steinvurzel P, Schonbrun E, Dan Y, Ellenbogen T and Crozier K B (2011); Multicolored vertical silicon nanowires; Nano Lett.; 11, 1851–1856.
13. Yin Y, Sun Y, Yu M, Liu M, Jiang T, Yang B, Liu B, Liu S and Cao W (2014); ZnO nanorod array grown on Ag layer: a highly efficient fluorescence enhancement platform; Scient. Rep.; 5, 8152.
14. Golde T E, Eckman C B, and Younkin S G (2000); Biochemical detection of Aβ isoforms: implications for pathogenesis, diagnosis, and treatment of Alzheimer's disease; Biochim. Biophys. Acta; 1502, 172–187.
15. Xia W, Yang T, Smith I.M., Shen Y.,Walsh D.M., Selkoe D.J. (2009); A Specific ELISA for Measuring Amyloid β-Protein Oligomers in Human Plasma and the Brains of Alzheimer Patients. Arch. Neurol. ; 66, 190–199.

ACCEPTED MANUSCRIPT

16. Xing Y and Xia N (2015); Biosensors for the determination of amyloid-beta peptides and their aggregates with application to alzheimer's disease; Anal. Lett.; 48, 879-893.
17. Sen J W, Bergen H R and Heegaard N H H (2003); On-line immunoaffinity-liquid chromatography-mass spectrometry for identification of amyloid disease markers in biological fluids; Anal. Chem; 75, 1196–1202.
18. Watanabe K C, Ishikawa H, Kuwahara K, Sato S, Komuro T, Nakagawa N, Nomura S, Watanabe and Yabuki M (2012); A new methodology for simultaneous quantification of total-Aβ, Aβx-38, Aβx-40, and Aβx-42 by columns witching LC/MS/MS; Anal. Bioanal. Chem; 402, 2033–2042.
19. Solé-Domènech S B, Johansson M, Schalling J Malm and Sjövall P (2010); Analysis of opioid and amyloid peptides using time-of-flight secondary ion mass spectrometry; Anal. Chem; 82. 1964–1974.
20. Inoue K D, Hosaka N, Mochizuki H, Akatsu K, Tsutsumiuchi Y, Hashizume N, Matsukawa T, Yamamoto and Toyo'oka T (2014); Simultaneous determination of posttranslational racemization and isomerization of N-terminal Amyloid-β in Alzheimer's brain tissues by covalent chiral derivatizedultraperformance liquid chromatography tandem mass spectrometry; Anal. Chem; 86, 797–804.
21. Positron Emission Tomography (PET) Drug SPL by U.S. Food and Drug Administration, https://www.fda.gov/ForIndustry/DataStandards/StructuredProductLabeling/ucm241316.htm
22. Ikonomovic M D, Klunk W E, Abrahamson E E, Mathis C A, Price J C, Tsopelas N D, Lopresti B J, Ziolko S, Bi W, Paljug W R, Debnath M L, Hope C E, Isanski B A, Hamilton R L and DeKosky S T (2008); Post-mortem correlates of in vivo PiB-PET amyloid imaging in a typical case of Alzheimer's disease; Brain; 131, 1630–1645.

ACCEPTED MANUSCRIPT

23. Pradhan N, Jana D, Ghorai BK, Jana NR (2012); Detection and Monitoring of Amyloid Fibrillation Using a Fluorescence "Switch-On" Probe. ACS Appl Mater Interfaces. 7(46):25813-20.

24. Chaudhary N, Singh S and Nagaraj R 2011 Aggregation properties of a short peptide that mediates amyloid fibril formation in model proteins unrelated to disease. J. Biosci. 36 679–689.

25. Groenning M (2010); Binding modeofThioflavin T and other molecular probes in the context of amyloid fibrils-current status; J Chem Bio; 3, 1-18.

26. Biancalana M, Makabe K, Koide A and Koide S (2009); Molecular mechanism of thioflavin-T binding to the surface of beta-rich peptide self-assemblies; J. Mol. Biol.; 385, 1052–1063.

27. Chitvoranund N, Jiemsirilers S and Kashima D P (2013); Effects of surface treatments on adhesion of silver film on glass substrate fabricated by electroless plating; J.Austra.Cer. Soc.; 49, 62 – 69.

28. Koura N (1990); Electroless plating of silver. In Electroless Plating: Fundamentals and Applications; William Andrew Publishing, LLC, New York, USA; 441-462.

29. Ghorbani H R, Mehir F P, Pazoki H and Rahamani M (2015); Synthesis of ZnO nanoparticles by precipitation method; Orient. J. Chem;31, 1219-1221.

30. Girigoswami K., Meenakshi V., Murugesan R. & Girigoswami A. (2015); Studies on Polymer-Coated Zinc Oxide Nanoparticles: UV-blocking Efficacy and in vivo Toxicity; Mater. Sci. Eng. C., 56: 501-510.

ACCEPTED MANUSCRIPT

31. Ibupoto Z H , Khun K, Eriksson M, AlSalhi M, Atif M, Ansari A and Willander M (2013); Hydrothermal growth of vertically aligned ZnO nanorods using a biocomposite seed layer of ZnO nanoparticles;Materials;6, 3584-3597.
32. Khun K, Ibupoto Z H, AlSalhi M, Atif M, Ansari A A and Willander M (2013); Fabrication of well-aligned znonanorods using a composite seed layer of ZnO nanoparticles and chitosan polymer; Materials; 6, 4361-4374.
33. Metkar S.K., Girigoswami A., Murugesan R. & Girigoswami K. (2017); In vitro and in vivo insulin amyloid degradation mediated by Serratiopeptidase; Mater. Sci. Eng. C.; 70:728-735.
34. Girigoswami K, Ku S H, Ryu J and Park C B (2008); A synthetic amyloid lawn system for high-throughput analysis of amyloid toxicity and drug screening; Biomaterials; 29, 2813-2819.
35. Parfenov A, Gryczynski I, Malicka J, Geddes C D and Lakowicz J R (2003); Enhanced fluorescence from fluorophores on fractal silver surfaces; J. Phys. Chem. B;107, 8829–8833.
36. Geddes C D, Parfenov A and Lakowicz J R (2003); Roughened silver electrodes for use in metal-enhanced fluorescence; Appl.Spectrosc.; 57, 526–531.
37. Gong J, Dai R C, Zhongping W and Zhang Z (2015); Thickness dispersion of surface plasmon of Ag nano-thin films: determination by ellipsometry iterated with transmittance method; Scien. Rep.; 5, 9279.
38. Sun Y, Wang L, Yu Y and Chen K (2012); Facile synthesis of flower-like 3D ZnO superstructures via solution route; Cryst. Eng. Comm.; 14, 3199-3204.
39. Wahab R, Kim S-Y, Mishra A, Yun S-I and Shin H S (2010); Formation of ZnO micro-flowers prepared via solution process and their antibacterial activity; Nanoscale Res Lett; 5, 1675–1681.

ACCEPTED MANUSCRIPT

40. Wang X, Song J and Wang Z L (2007); Nanowire and nanobelt arrays of zinc oxide from synthesis to properties and to novel devices; J. Mater. Chem; 17, 711–720.

41. Wang C, Mao M, Wang N, Kang Z and Tian C (2007); Solution synthesis of ZnO nanotubes via a template-free hydrothermal route; Solid StateCommun.; 141, 620–623.

42. Wang T, Costan J, Centeno A, Pang J S, Darvill D, Ryana M P and Xie F (2015); Broadband enhanced fluorescence using zincoxide nanoflower arrays; J. Mater. Chem. C; 3, 2656–2663

43. Lukomska J, Malicka J, Gryczynski I, Leonenko Z andLakowicz J R (2005); Fluorescence Enhancement of Fluorophores Tethered to DifferentSized Silver Colloids Deposited on Glass Substrate; Biopolym.; 77, 31–37.

44. Borner S, Ruter C E, Voss T, Kip D, and Schade W (2007); Modeling of ZnO nanorods for evanescent field optical sensors; Phys. Stat. Sol.; 204, 3487–3495.

45. Voss T, Svacha G T and Mazur E (2007); High-order waveguide modes in ZnO nanowires. Nano Lett.; 7, 3675–3680.

ACCEPTED MANUSCRIPT

ACCEPTED MANUSCRIPT

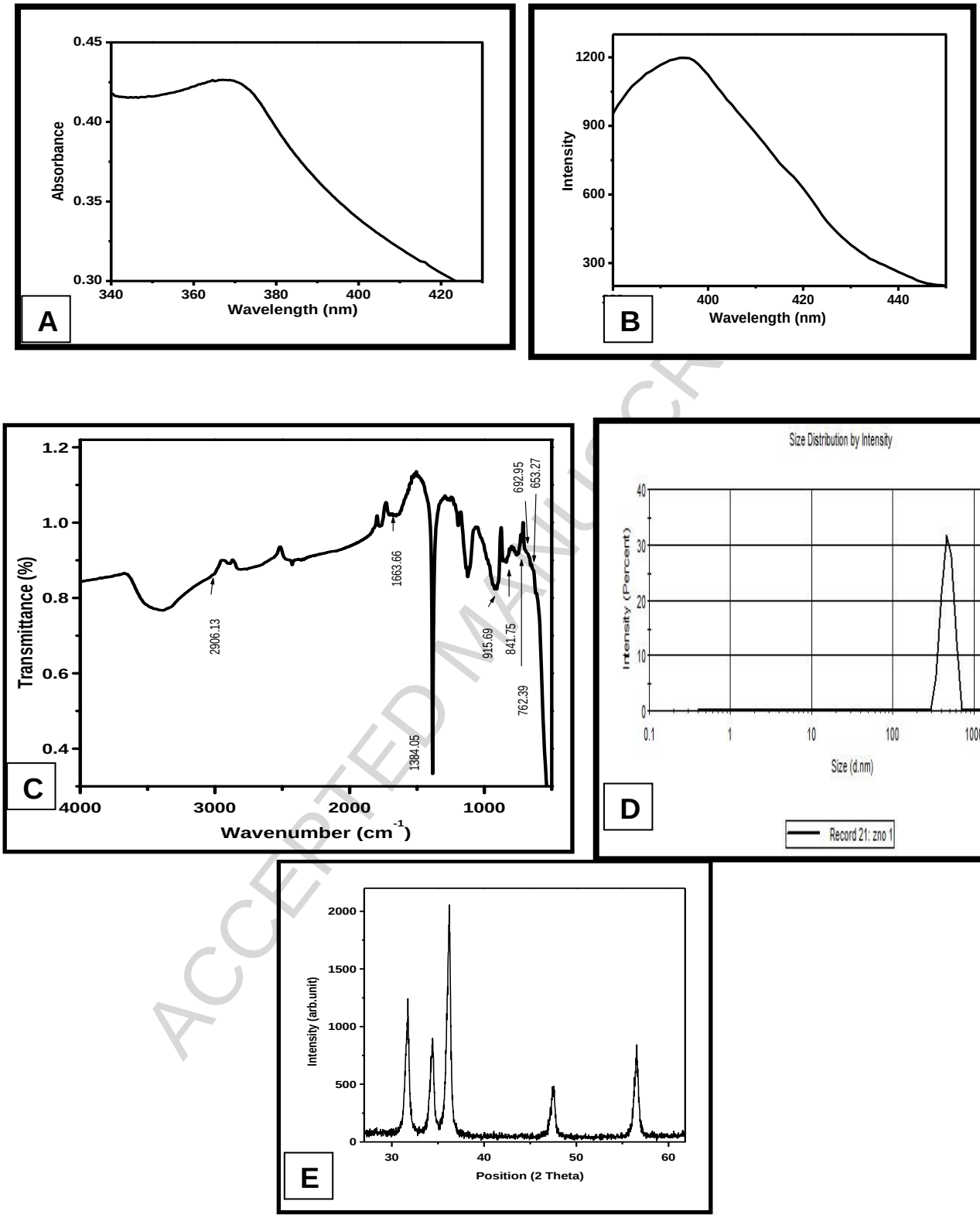

Fig-1: Characterization of zinc oxide nanoparticles (ZnO NPs) synthesized to be used as a seed for ZnO NF growth. (A) UV – visible spectrum. (B) Fluorescence emission spectrum. (C) Fourier Transform Infrared (FTIR) spectrum. (D) Hydrodynamic diameter using particle size analyzer. (E) X-ray diffraction analysis.

ACCEPTED MANUSCRIPT

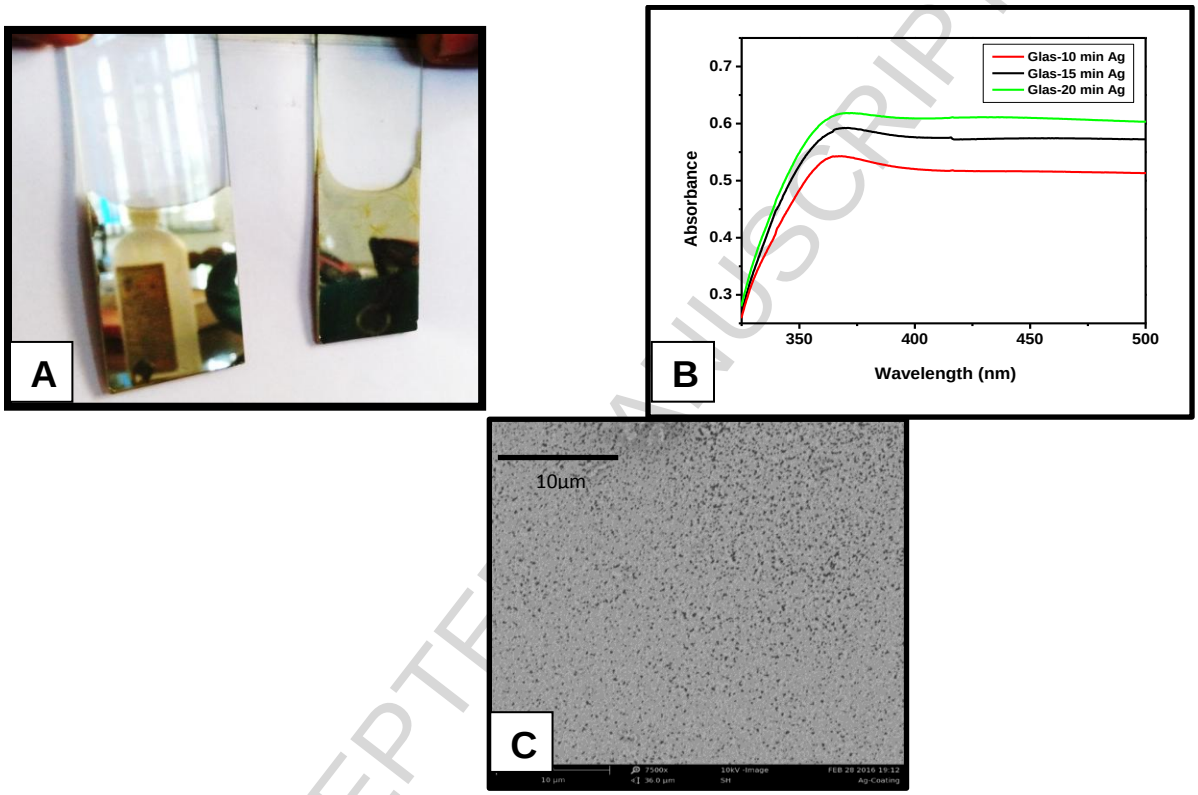

Fig-2: Electroless deposition of nano silver (Ag) on activated glass slide and characterization. (A) The silver (Ag) thin film coating was done using simple wet chemistry yielding a fine Ag mirror on activated glass substrate. (B) UV-visible spectroscopy confirms the Ag thin film coating and (C) the morphology of thin film was determined by the Scanning Electron Microscope (SEM).

ACCEPTED MANUSCRIPT

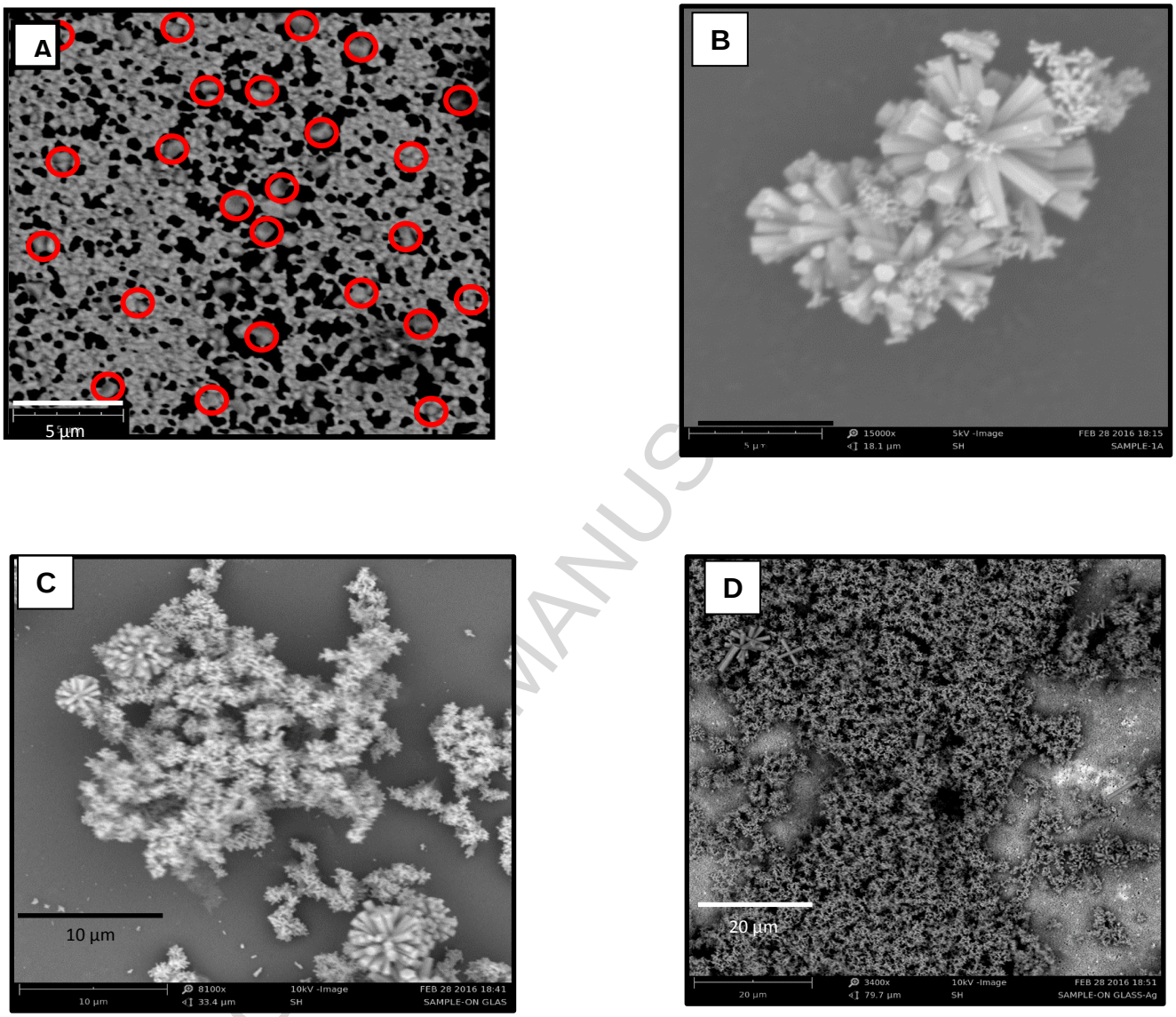

Fig-3: SEM images of different stages of the engineered substrate. (A).Seed layer deposition of ZnO NPs (red circles) on activated glass substrate (12, 000X magnification). (B) ZnO NF etched out from activated glass surface (15, 000 X magnification). (C) ZnO NF grown on activated glass surface (8100 X magnification). (D) ZnO NF grown on nano Ag thin film coated glass surface (3400 X magnification).

ACCEPTED MANUSCRIPT

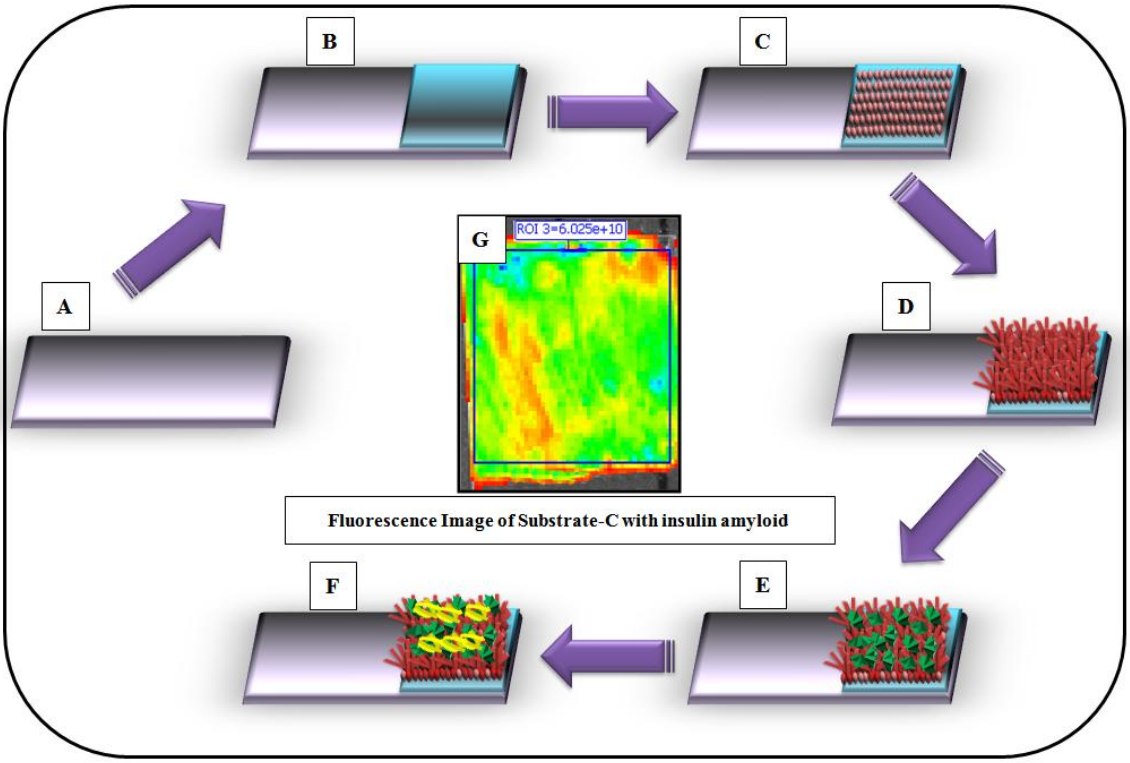

Fig-4: Schematic representation of amyloid sensor fabrication. (A) Glass slide activation, (B) Nano Ag thin film coating, (C) To this coated slide, synthesized ZnO NPs were spin coated and (D) ZnO NFs were grown. (E) Then our target fluorophore ThT is adsorbed over the ZnO NFs and (F) the analyte (insulin amyloid) were adsorbed into it. (G) The fluorescence image was acquired using Lumina IVIS.

ACCEPTED MANUSCRIPT

ACCEPTED MANUSCRIPT

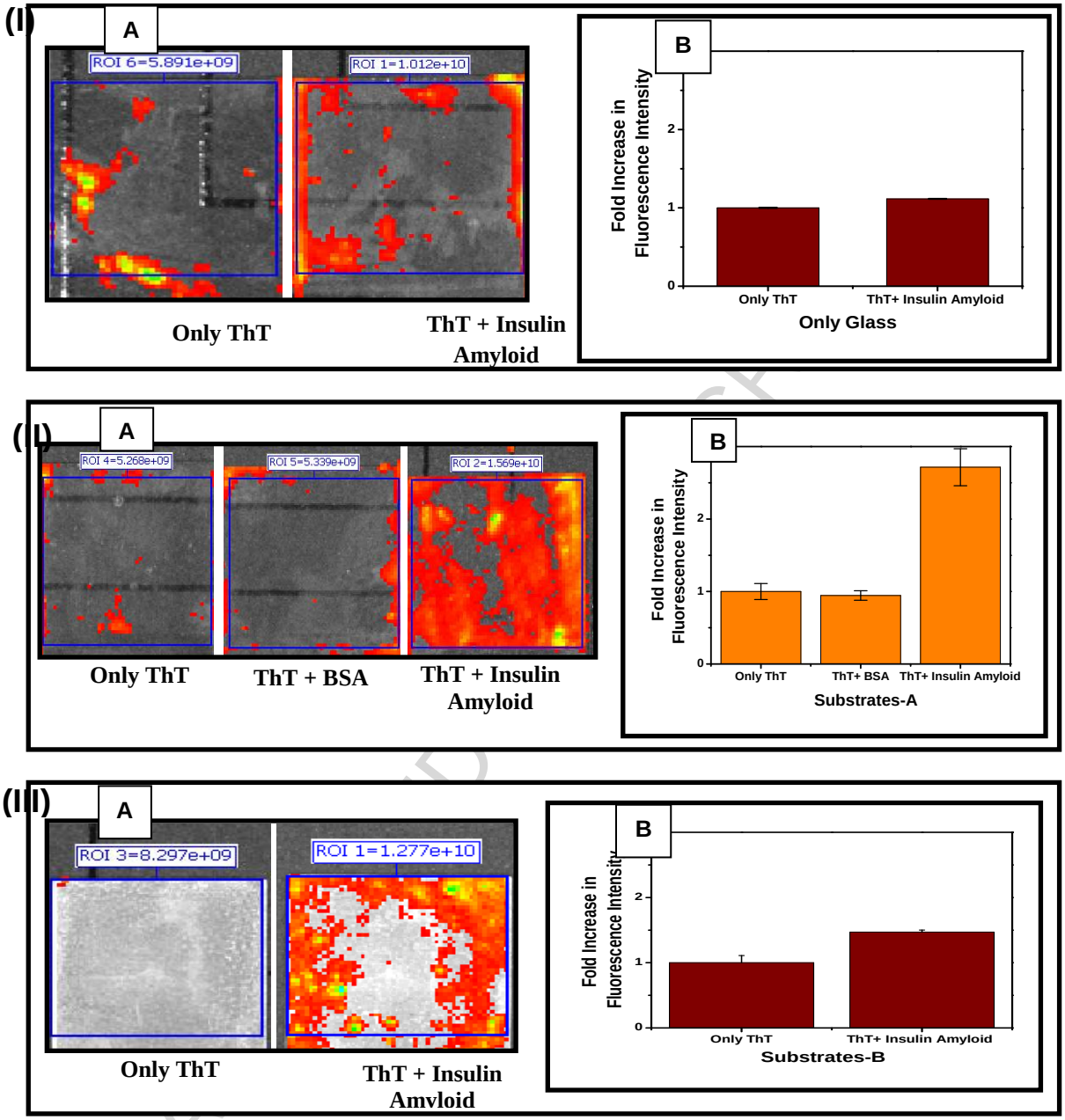

ACCEPTED MANUSCRIPT

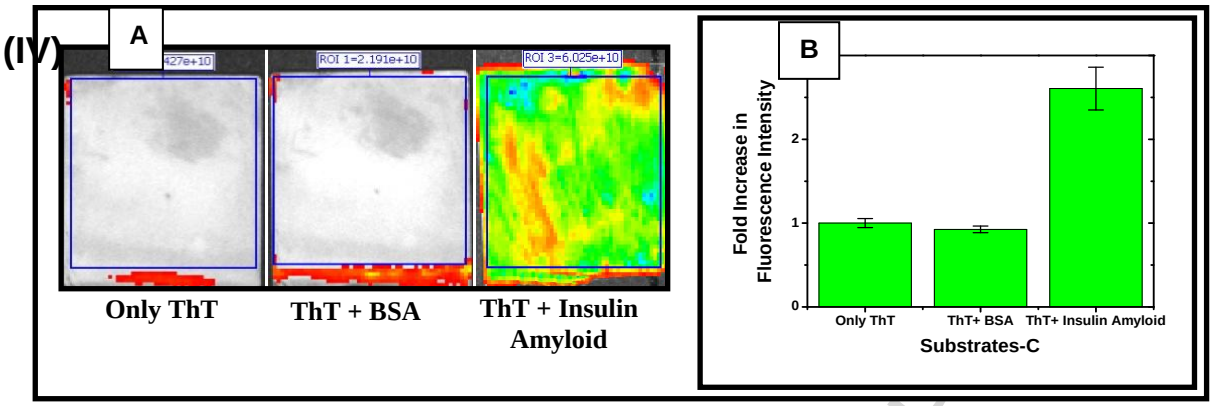

Fig-5: Insulin amyloid detection using various substrates. The insulin amyloid (10 µl of 1.388 mg/ml) was used as model amyloid protein and BSA was taken as negative control. The fluorescence image captured by Lumina IVIS of various substrates (panel A) and the fold increase in fluorescence intensity recorded by using ROI (region of interest) tool (panel B) for (I) Only Glass (activated glass slide), (II) Substrate-A (ZnO NFs grown on activated glass slide), (III) Substrate-B (Ag coated glass slide) and (IV) Substrate-C (ZnO NFs grown on Ag coated glass slide).

ACCEPTED MANUSCRIPT

ACCEPTED MANUSCRIPT

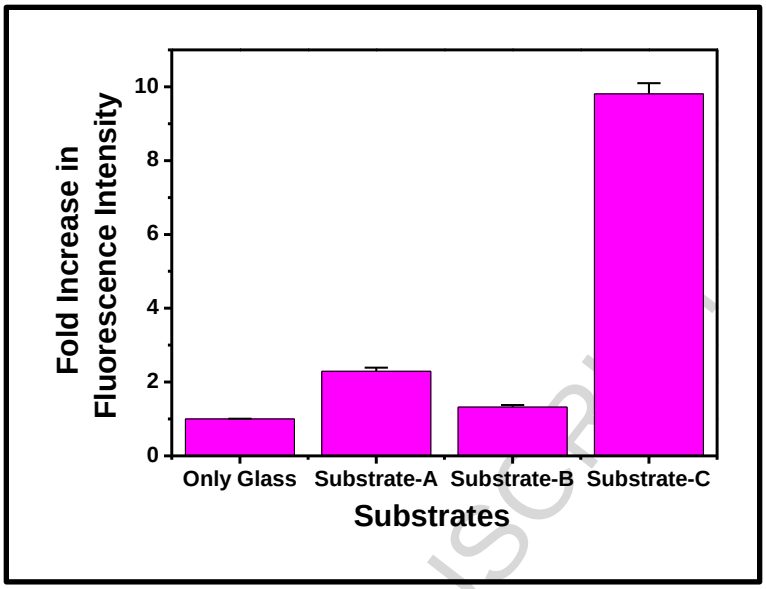

Fig-6: Fold increase in fluorescence intensity from different substrates. In the various substrates same amount (10 µl of 1.388 mg/ml) of insulin amyloid was given and fluorescence images were interpreted. It was observed that the maximum fluorescence intensity was produced by Substrate-C. Compared to Only Glass, 9.81±0.29 fold higher fluorescence signals were produced by Substrate-C.

ACCEPTED MANUSCRIPT

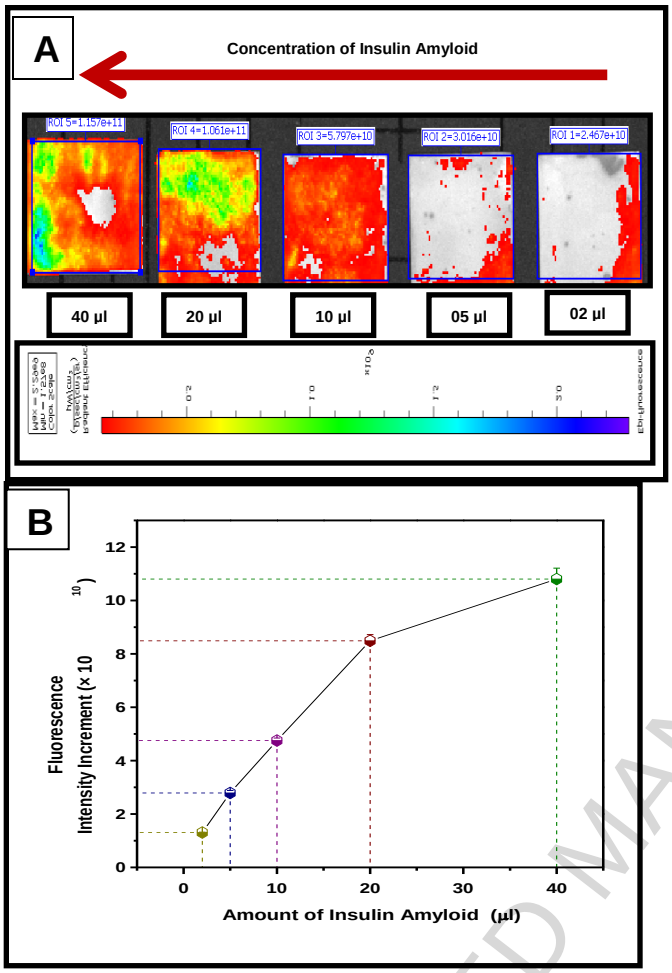

Fig-7: Linearity of Substrate-C as amyloid sensor. (A) The fluorescent images of Substrate C studied using Lumina IVIS after addition of different amount of insulin amyloid. (B) Fluorescence intensity for different amounts of insulin amyloid were plotted.

ACCEPTED MANUSCRIPT

Highlights

Amyloids are responsible for different neurodegenerative diseases; its detection is important for early diagnosis.

Conventional methods are expensive and time consuming

Present study demonstrates a ZnO nanoflower grown on nano Ag thin film based nanobiosensor for amyloid detection

ACCEPTED MANUSCRIPT